

Relativistic hybrid stars in light of the NICER PSR J0740 + 6620 radius measurement

Jia Jie Li^{*}

School of Physical Science and Technology, Southwest University, Chongqing 400700, China

Armen Sedrakian[†]

*Frankfurt Institute for Advanced Studies, D-60438 Frankfurt am Main, Germany
and Institute of Theoretical Physics, University of Wrocław, 50-204 Wrocław, Poland*

Mark Alford[‡]

Department of Physics, Washington University, St. Louis, Missouri 63130, USA

 (Received 13 September 2021; accepted 10 November 2021; published 21 December 2021)

We explore the implications of the recent radius determination of PSR J0740 + 6620 by the NICER experiment, combined with the neutron skin measurement by the PREX-II experiment and the associated inference of the slope of symmetry energy, for the structure of hybrid stars with a strong first-order phase transition from nucleonic to quark matter. We combine a covariant density-functional nucleonic equation of state (EOS) with a constant-speed-of-sound EOS for quark matter. We show that the radius and tidal deformability ranges obtained from GW170817 can be reconciled with the implication of the PREX-II experiment if there is a phase transition to quark matter in the low-mass compact star. In the high-mass segment, the EOS needs to be stiff to comply with the large-radius inference for PSR J0740 + 6620 and J0030 + 0451 with masses $M \simeq 2 M_{\odot}$ and $M \simeq 1.4 M_{\odot}$. We show that twin stars are not excluded, but the mass and radius ranges (with $M \geq M_{\odot}$) are restricted to narrow domains $\Delta M_{\text{twin}} \lesssim 0.05 M_{\odot}$ and $\Delta R_{\text{twin}} \sim 1.0$ km. We also show that the existence of twin configurations is compatible with the light companion in the GW190814 event being a hybrid star in the case of values of the sound-speed square $s = 0.6$ and $s = 1/3$.

DOI: [10.1103/PhysRevD.104.L121302](https://doi.org/10.1103/PhysRevD.104.L121302)

I. INTRODUCTION

The recent mass measurement of the heaviest pulsar to date, PSR J0740 + 6620 [1], which is currently at $2.08^{+0.07}_{-0.07} M_{\odot}$, and the recent analysis [2,3] of x-ray data from the NICER experiment, which gave the radius estimates $12.39^{+1.30}_{-0.98}$ km [2] and $13.71^{+2.61}_{-1.50}$ km [3] and the corresponding mass estimates $2.07^{+0.07}_{-0.07} M_{\odot}$ and $2.08^{+0.09}_{-0.09} M_{\odot}$ of PSR J0740 + 6620, open prospects of constraining the properties of the dense-matter equation of state (EOS)—in particular, the possibility of a phase transition at high densities.

The lower bound on the radius of PSR J0740 + 6620 constrains a highly relevant region of the mass-radius (M - R) diagram of compact stars (CSs), which in combination with the determination of the tidal deformability (TD) of a star of mass $\sim 1.4 M_{\odot}$ in the GW170817 event by the LIGO-Virgo Collaboration [4], puts significant constraints on the EOSs of CSs. These require that the stellar

EOS must be moderately soft at intermediate densities (to allow for relatively small TDs) and must be stiff enough at high densities (to allow for two-solar-mass CSs; see Refs. [5–11]).

Recently, the Lead Radius Experiment Collaboration (PREX-II) reported the most precise measurement yet of the neutron skin thickness of the lead nucleus, $R_{\text{skin}}^{208} = 0.283 \pm 0.071$ fm (mean and 1σ standard deviation), in a parity-violating electron scattering experiment [12]. Subsequent theoretical analysis [13,14] based on density-functional theory established values of the symmetry energy E_{sym} and the slope of nuclear symmetric energy L_{sym} at saturation density (ρ_{sat}) that are consistent with the inferred value of R_{skin}^{208} . Reference [13] finds $E_{\text{sym}} = 38.1 \pm 4.7$ MeV and $L_{\text{sym}} = 106 \pm 37$ MeV from a family of relativistic (nonlinear, meson-exchange) density functionals (DFs). Reference [14] expanded the base (and the functional form) of employed DFs to include nonrelativistic DFs, relativistic DFs with density-dependent meson-exchange couplings, and relativistic point coupling DFs to find $E_{\text{sym}} = 32 \pm 1$ MeV and $L_{\text{sym}} = 54 \pm 8$ MeV. These values include the additional requirement on DFs

^{*}jiajieli@swu.edu.cn

[†]sedrakian@fias.uni-frankfurt.de

[‡]alford@physics.wustl.edu

to be consistent with the experimental limits on the dipole polarizability of ^{208}Pb , which prefer DFs predicting a small value of L_{sym} . The large value of L_{sym} found in the first analysis is in potential tension with the various estimates [15–18], whereas the value obtained from the second analysis is within the range inferred previously. Note that the difference between the two quoted values of L_{sym} is 1.37σ , which translates to about 83% significance. Since L_{sym} is highly correlated with the stellar radius and TD, the rather large value found in the first analysis is in potential tension with the GW170817 deformability measurement if one assumes a purely nucleonic composition [13].

Nevertheless, independent of the interpretation of the PREX-II experiment, the potential tension outlined above suggests a close examination of the compatibility of a large value of L_{sym} with the constraints on compact stars. Here we address the possibility of *first-order phase transition* from nucleonic to quark matter using (a) the radius measurements of two neutron stars by NICER, (b) the TD of GW170817, and (c) a range of values of L_{sym} suggested by Refs. [13,14].

The composition of matter at high densities achieved in a CS’s core remains unknown. One possibility is a deconfinement phase transition from bound states of hadrons to liberated quark states [19]. If the quark matter in a CS’s core is relatively soft, then its radius and TD are reduced, which could avoid the tentative tension between the inferred TDs from the GW170817 event and those predicted by purely hadronic stiff EOS models without a phase transition [20–34]. Of particular interest in this scenario is the emergence of *twin and triplet stars*, where one (or two) hybrid stars have the same mass as, but a different radius

from, a purely hadronic star [21,25–27,30,35,36]. The more extreme case of triplets will not be discussed here.

With a mass of about $2.1 M_{\odot}$, PSR J0740 + 5620 is the most massive known CS: it is about 50% more massive than PSR J0030 + 0451. Yet, current measurements do not indicate a significant difference in size; see Fig. 1. As mentioned earlier, the generic feature of the first-order phase transition is the softening of the EOS in the vicinity of the transition point, which leads to smaller radii of hybrid stars as compared to the nucleonic ones. Confronting the very massive star’s radius estimation with the possible phase transition in dense matter is thus very timely. This issue has been discussed by Refs. [5,7].

In this work, we apply the setup developed by us earlier [30] to explore the consequences of a strong first-order phase transition from nucleonic to quark matter and the formation of twin stars. The resulting models are then confronted with the newly available data from NICER and PREX-II experiments.

II. CONSTRUCTION OF EOS

To describe low-density matter, we use a covariant density functional (CDF) of nuclear matter in which baryons are coupled to mesons with density-dependent couplings, and we adopt as a reference the DDME2 parametrization [39]. The CDF EOS models can be extended by modifying the density dependence of the couplings [40] such as to map the CDF EOS models onto purely phenomenological ones [41], which are based on an expansion of the energy density of nuclear matter close to the saturation density ρ_{sat} with respect to the density and isospin asymmetry—i.e.,

$$E(\chi, \delta) \simeq E_{\text{sat}} + \frac{1}{2!} K_{\text{sat}} \chi^2 + \frac{1}{3!} Q_{\text{sat}} \chi^3 + E_{\text{sym}} \delta^2 + L_{\text{sym}} \delta^2 \chi + \mathcal{O}(\chi^4, \chi^2 \delta^2), \quad (1)$$

where $\chi = (\rho - \rho_{\text{sat}})/3\rho_{\text{sat}}$, with ρ and ρ_{sat} being the number density and its value at saturation, and $\delta = (\rho_n - \rho_p)/\rho$, where $\rho_{n(p)}$ is the neutron (proton) number density. The coefficients of the expansion are known as the *incompressibility* K_{sat} , the *skewness* Q_{sat} , the *symmetry energy* E_{sym} , and the *slope parameter* L_{sym} . In this manner, the uncertainties in the gross properties of CSs can be quantified in terms of not-well-known higher-order characteristics of nuclear matter, specifically Q_{sat} and L_{sym} [40,41]. The low-order characteristics are fixed at their values predicted by the DDME2 parametrization: $E_{\text{sat}} = -16.14$, $K_{\text{sat}} = 251.15$, $E_{\text{sym}} = 32.31$ MeV, and $\rho_{\text{sat}} = 0.152 \text{ fm}^{-3}$. At the same time, the CDF provides access to the composition of matter which is not fixed in agnostic models based on nuclear characteristics only.

Motivated by this, we construct six representative EOSs featuring combinations of three values of $Q_{\text{sat}} = -500$,

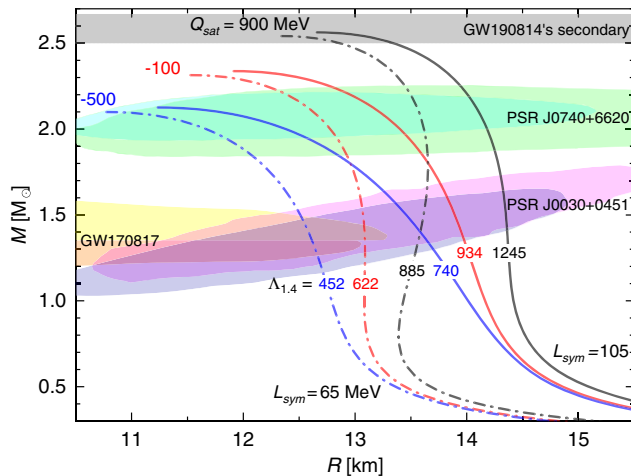


FIG. 1. M - R relation for nucleonic EOS for different pairs of values of Q_{sat} and L_{sym} . In addition, we show the TD of a canonical-mass CS for each model. Constraints with 90% credibility from multimessenger astronomy are shown by shaded regions [2–4,37,38]; see text for details.

–100, 900 MeV and two values of $L_{\text{sym}} = 65, 105$ MeV. The value of Q_{sat} controls the high-density behavior of the EOSs, and thus, the maximum mass of a static CS [40]. For $Q_{\text{sat}} = -500$ MeV, the maximum mass is about $2.1 M_{\odot}$, which matches the mass measurement of PSR J0740 + 6620 [1,42]; for $Q_{\text{sat}} = -100$ MeV, the maximum mass is consistent with the (approximate) *upper limit* on the maximum mass of static CSs $\sim 2.3 M_{\odot}$ inferred from the analysis of the GW170817 event [43,44]; finally, for $Q_{\text{sat}} = 900$ MeV, the maximum mass is close to $2.5 M_{\odot}$, which would be compatible with the mass of the secondary in the GW190814 event [45] and its interpretation as a nucleonic CS [46,47]. We choose values of L_{sym} corresponding to the central value and the lower range of the 1σ confidence interval (CI) of the PREX-II measurement, $L_{\text{sym}} = 106 \pm 37$ MeV [12,13]. Note that the recent measurement of the spectra of pions in intermediate energy collisions implies $L_{\text{sym}} = 79.9 \pm 37.6$ MeV [48]. In addition, an analysis based on nonparametric EOSs shows that there is a mild tension between the results of Ref. [13] and astrophysical data supplemented by chiral effective field theory results [49].

The M - R relations for our six EOSs are shown in Fig. 1, where we also show the current astrophysical observational constraints. We show 90%-credible ellipses from each of the two NICER modeling groups for PSR J0030 + 0451 and J0740 + 6620 [2,3,37,38]. We also show 90%-credible regions for each of the two CSs that merged in the gravitational wave event GW170817 [4]. Finally, we show the 90% CI for the mass of the secondary component of GW190814 [45]. A lower limit on the average TD $\tilde{\Lambda}_{1.186} \geq 240$ (with binary chirp mass $\mathcal{M} = 1.186 M_{\odot}$) was extracted from the GW170817 event using the observations and modeling of this merger [50,51]. This limit allows for hybrid stars having $R_{1.4}$ radii [24] well below the corresponding NICER limits [37,38].

The softest EOS model ($Q_{\text{sat}} = -500$, $L_{\text{sym}} = 65$ MeV), which gives $R_{1.4} = 12.58$ km and $\Lambda_{1.4} = 452$ for a canonical-mass star, appears as the only model satisfying all three of the M - R constraints. The stiffest EOS model ($Q_{\text{sat}} = 900$, $L_{\text{sym}} = 105$ MeV), which gives $R_{1.4} = 14.37$ km and $\Lambda_{1.4} = 1245$, passes through the upper range of the CIs provided by NICER results. The M - R relations shown in Fig. 1 indicate that one could find a compromise between the requirements of a soft EOS (from GW170817) and the relatively large value of L_{sym} implied by the analysis of PREX-II in Ref. [13]. This would be accomplished by an EOS with $L_{\text{sym}} \sim 65$ MeV, which is at the lower end of the 1σ range of Ref. [13], and a negative Q_{sat} .

So far, we have seen that fairly low values of L_{sym} from the range consistent with the inference [13] from the PREX-II experiment allow us to build models that are consistent with the known astronomical constraints. However, as we show next, larger values from the experimental range of L_{sym} can be accommodated if a strong

first-order phase transition to quark matter is allowed for. We will model below the EOS of the quark phase using the constant-sound-speed (CSS) parametrization [35,52], which matches well with the predictions based on the Nambu–Jona-Lasinio (NJL) model computations which include vector repulsion [53,54]. We assume a first-order phase transition with a sharp boundary between the nucleonic and quark phases (which is the case when mixed phases are disfavored by surface tension and electrostatic energy costs [55]). The pressure is then given by [35,52]

$$p(\varepsilon) = \begin{cases} p_{\text{tran}}, & \varepsilon_{\text{tran}} < \varepsilon < \varepsilon_{\text{tran}} + \Delta\varepsilon, \\ p_{\text{tran}} + s[\varepsilon - (\varepsilon_{\text{tran}} + \Delta\varepsilon)], & \varepsilon_{\text{tran}} + \Delta\varepsilon < \varepsilon, \end{cases} \quad (2)$$

where p_{tran} is the transitional pressure with energy density $\varepsilon_{\text{tran}}$, $\Delta\varepsilon$ is the discontinuity, and s is the square of the sound speed in the quark phase. The possible topologies of hybrid stars in the M - R diagram based on CSS parametrization have been studied [35]. Of particular interest is the case where, by an appropriate choice of the parameters p_{tran} , $\Delta\varepsilon$, and s , there are two disconnected branches of stars: one with purely nucleonic and the other with hybrid stars. Such topology leads, in particular, to twin configurations where stars have identical masses but different radii [21,25–27]. The more extreme case of three disconnected branches leads to the formation of triplets, which will not be studied here [36].

Figure 2 illustrates how such a transition to quark matter allows a nuclear EOS with a large L_{sym} to be consistent

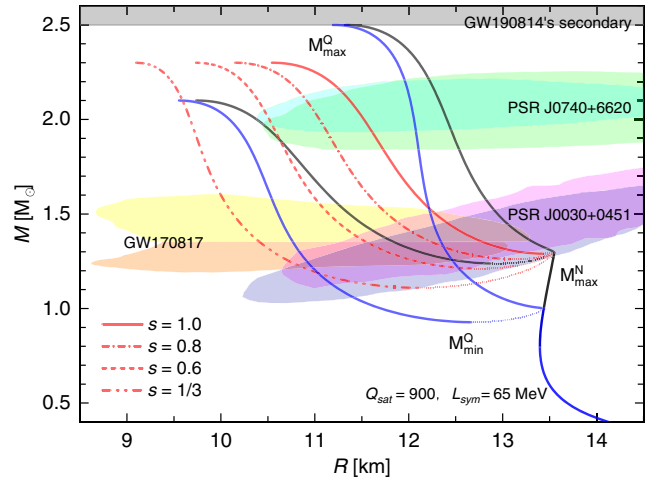


FIG. 2. Illustrative M - R relation for hybrid EOS models. The results are constructed by varying one of the three quantities that fully determine the model at fixed values of the two others. These are the maximum masses of the quark $M_{\text{max}}^{\text{Q}}$ and nucleonic $M_{\text{max}}^{\text{N}}$ branches and the sound-speed square s . The dotted thin lines indicate unstable configurations. All the solid curves correspond to $s = 1.0$. For the remaining curves, the value of s is as indicated in the plot.

with astrophysical constraints. We have fixed the nuclear EOS by choosing $L_{\text{sym}} = 65$ and $Q_{\text{sat}} = 900$ MeV. We vary the CSS parameters of the quark-matter EOS to explore different sound speeds s , and by varying ρ_{tran} and $\Delta\varepsilon_{\text{tran}}$ we can explore different values of the maximum masses $M_{\text{max}}^{\text{N}}$ and $M_{\text{max}}^{\text{Q}}$ on the nucleonic branch and hybrid branch, respectively. In particular, each of the two same-color solid lines differ only by the value of $M_{\text{max}}^{\text{Q}}$.

The sequences shown in Fig. 2 are for $M_{\text{max}}^{\text{Q}}/M_{\odot} = 2.1, 2.3, 2.5$ and $M_{\text{max}}^{\text{N}}/M_{\odot} = 1.0, 1.3$ (corresponding to transition densities $\rho_{\text{tran}}/\rho_{\text{sat}} = 1.81, 2.05$). We see that a stiff nucleonic EOS can be made compatible with the GW170817 constraint if there is a first-order transition to quark matter at densities $\rho_{\text{tran}} \lesssim 2\rho_{\text{sat}}$.

Figure 2 shows, in addition, the sensitivity of results toward varying the value of s for a specific case with fixed maximum masses. Since a reduction of s from its maximal value softens the quark-matter EOS, the M - R curves are shifted to the left, eventually putting some of them ($s \lesssim 0.6$) outside of the NICER result for PSR J0740 + 6620. Note that in Fig. 2, two topologies of M - R curves are present: the

connected and disconnected ones, the latter having a region of instability between the nucleonic and hybrid configurations. In the following, we focus on the disconnected topologies.

III. MASS-RADIUS CONSTRAINT FOR HYBRID STARS

To study the occurrence of twin configurations, we select EOSs from the parameter space of our model that have twin configurations and are consistent with both NICER and gravitational wave measurements. Specifically, they yield radii that are above the NICER 90%-confidence lower limit from PSR J0740 + 6620 and J0030 + 0451, and below the 90%-confidence upper limit on the radius of a $1.36 M_{\odot}$ star from the GW170817 event; (the stellar mass is chosen to be the one inferred for an equal-mass binary.) Figure 3 shows examples of our exploration of this parameter space. Each of the six panels in Fig. 3 has curves for two nuclear EOSs (with the values of L_{sym} and Q_{sat} given in each panel title) and a fixed speed of sound in the quark-matter EOS (also given in each panel title). Within each panel, we vary the

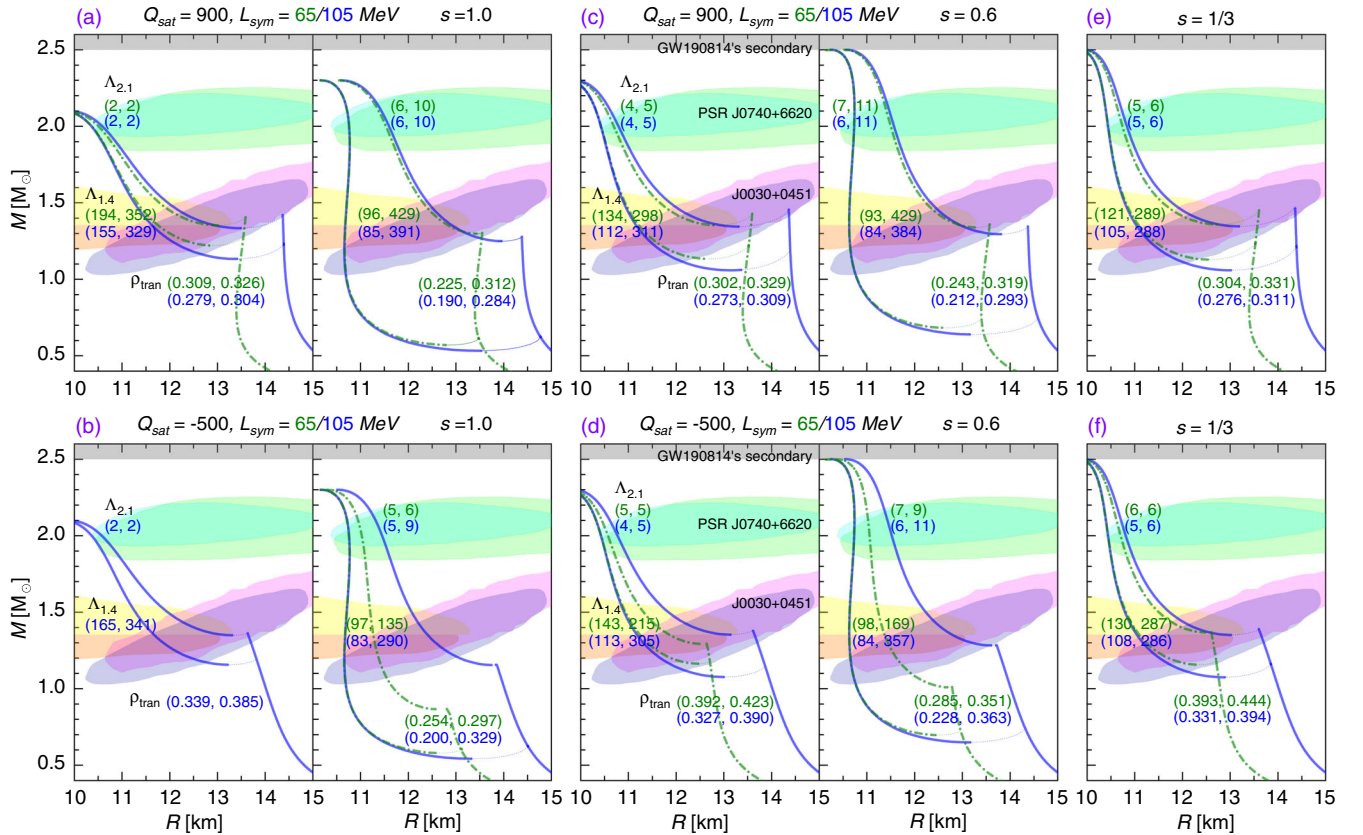


FIG. 3. Constraints on the M - R relation of CSs featuring twin configurations (in some cases, the instability region is not resolved on the figure's scale). Panels (a) and (b): M - R curves for hybrid stars characterized by different maximum masses (attained on the quark branch) for nucleonic EOSs with pairs of values of Q_{sat} (-500 and 900 MeV) and L_{sym} (65 and 105 MeV), and quark-matter CSS EOSs with $s = 1.0$ (in natural units). The ranges of transition density ρ_{tran} in units of fm^{-3} and the TDs $\Lambda_{1,4}$ and $\Lambda_{2,1}$ (dimensionless) for a canonical mass $M/M_{\odot} = 1.4$ and massive $M/M_{\odot} = 2.1$ stars, respectively, are quoted as well. The color coding of numbers matches that of the curves. Panels (c),(d) and (e),(f): same as in (a),(b), but with $s = 0.6$ and $s = 1/3$, respectively.

remaining parameters of the quark-matter EOS (the nuclear matter density at the transition ρ_{tran} and energy density jump at the transition $\Delta\epsilon$) as follows: In each of the one or two plots in each panel, we require the maximum mass on the hybrid branch $M_{\text{max}}^{\text{Q}}$ to have a different value (which can be read off from the y axis), and in each plot, we show results for two values of $M_{\text{max}}^{\text{N}}$ which span the range within which the M - R curves obey the mass-radius constraints as described in the previous paragraph, and contain twin stars (i.e., a discontinuity between the nuclear branch and the hybrid branch).

Let us first focus on the case $s = 1.0$ [Figs. 3(a) and 3(b)]. The following systematics are observed in our setup:

- (i) The stiffer the nucleonic EOS, the larger the range of masses and radii where twin stars exist; see also Fig. 4 below. Intuitively, this makes sense, as the stiffer nuclear EOS pushes the nucleonic branch to higher radii, further from the hybrid branch.
- (ii) The larger the value of $M_{\text{max}}^{\text{Q}}$, the narrower the range of masses where twins exist and the instability region between nucleonic and hybrid stars. A higher value, in the current setup, requires a smaller $\Delta\epsilon$ to

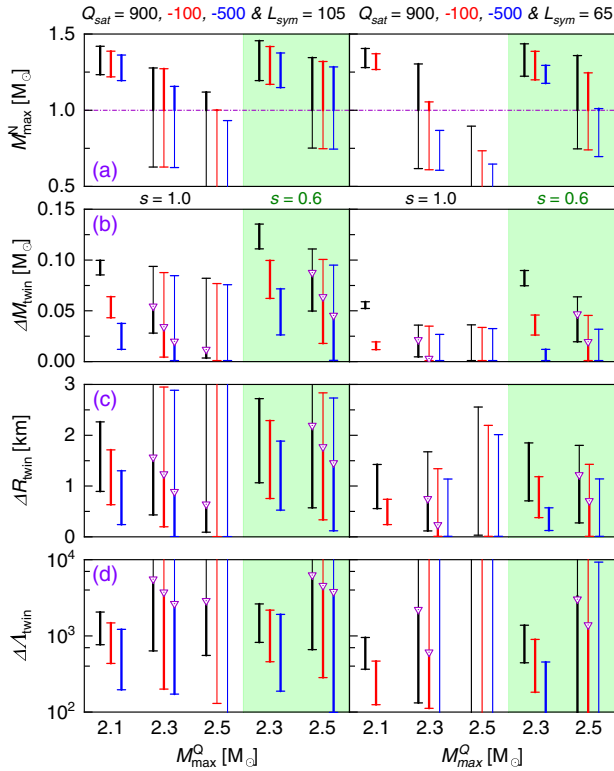


FIG. 4. Ranges of parameters $M_{\text{max}}^{\text{N}}$, ΔM_{twin} , ΔR_{twin} , and $\Delta\Lambda_{\text{twin}}$ characterizing twin configurations (see text for definitions) for EOSs constructed using nucleonic matter with pairs of values of Q_{sat} (-500 , -100 and 900 MeV) and L_{sym} (65 and 105 MeV) and quark matter with $s = 1.0$ and 0.6 (shadowed). The triangles followed by the thin lines correspond to twins with $M \leq 1.0 M_{\odot}$. See text for discussion.

allow for a steep increase of the mass. Since for our parameter choice the M - R curves pass through the GW170817 90%-credible region, the quoted values of TD are consistent with the upper limit set by the GW170817 on this quantity event [4].

Consider next the case of less stiff quark EOSs with $s = 0.6$ [Figs. 3(c) and 3(d)] and $s = 1/3$ [Figs. 3(e) and 3(f)]. The general features found above are replicated in this case as well. However, in this case we find twin solutions for models supporting heavier stars, with $M_{\text{max}}^{\text{Q}}/M_{\odot} \gtrsim 2.3$. Interestingly, the $M_{\text{max}}^{\text{Q}}/M_{\odot} = 2.5$ sequence, in which the light component in the GW190814 would be a hybrid star (see Fig. 3), allows for twin solutions for $s = 0.6, 1/3$ in the considered range $65 \leq L_{\text{sym}} \leq 105$ MeV. Compared to the $s = 1.0$ case for the same maximum mass $M_{\text{max}}^{\text{Q}}$, the value of $M_{\text{max}}^{\text{N}}$ is shifted upwards significantly, which promotes the appearance of twin configurations.

The analysis above shows, among other things, that NICER’s 90% CI for PSR J0740 + 6620 does not preclude a strong first-order phase transition, which (very robustly) leads to a shift of the radius toward smaller values compared to the case without phase transition. Furthermore, the fact that PREX-II analysis of Ref. [13] indicates $L_{\text{sym}} > 65$ MeV at a 68% confidence level and $L_{\text{sym}} > 45$ MeV at 90% corroborates the scenario of such a strong first-order phase transition, as a large L_{sym} allows for a large radius of the nucleonic low-mass stars and thus “leaves room” on the M - R diagram for a hybrid branch with a smaller radius that is consistent with astrophysical measurements. In such a scenario, the appearance of twin configurations is possible. This leads us to the conclusion that even the relatively low-mass $M/M_{\odot} \leq 1.5$ CSs could be, in fact, hybrid stars.

Figure 4 shows the values of $M_{\text{max}}^{\text{N}}$ for which twins arise; the mass range of twins ΔM_{twin} , defined as the range between $M_{\text{max}}^{\text{N}}$ and the minimum value of a CS mass on the hybrid branch; and the intervals of the radius ΔR_{twin} and TD $\Delta\Lambda_{\text{twin}}$ associated with this mass range, as functions of the parameters defining the EOS. For $s = 1.0$, twin configurations arise for $M_{\text{max}}^{\text{Q}}/M_{\odot} \lesssim 2.3$ (within the parameter space explored and excluding twins with $M < 1.0 M_{\odot}$; see below), but for $s = 0.6$, the values $M_{\text{max}}^{\text{Q}}/M_{\odot} \sim 2.5$ are obtained. This has implications for the GW190814 event, which involved a merger of a $23 M_{\odot}$ black hole with a $\sim 2.6 M_{\odot}$ object. Therefore, this object could have been a hybrid star living on a CS sequence which contains a twin—i.e., the GW190814 event does not exclude twins. (For a contrary view, see Ref. [56].)

In Fig. 4, we see that the range of masses containing twins is small, $\Delta M_{\text{twin}} \lesssim 0.05 M_{\odot}$. For radii, note that the triangles followed by thin lines denote twins with $M < 1.0 M_{\odot}$. This is a rough threshold below which stars are unlikely to be observed because of their likely instability at the proto-neutron star stage [57,58]. With that condition, the radius difference of twins is $\Delta R_{\text{twin}} \sim 1$ km

for $s = 1.0$; the difference is larger for $s = 0.6$, with ΔR_{twin} reaching up to 3 km. This range is largest for very stiff nucleonic EOSs, which predict a large radius. The narrow range of masses and the modest radius difference for twins is a consequence of the constraint imposed by the large radius of PSR J0740 + 662, which limits the allowed range of the reduction of the radius of a hybrid star and makes it challenging to distinguish between nucleonic and hybrid stars, as $\Delta R_{\text{twin}} = 1$ km requires radius measurement accuracy of less than 10%. However, the difference in the TDs of twins can be several hundred to two thousand—see Fig. 4(d)—therefore, studies of $\Lambda_1 - \Lambda_2$ extracted from the inspiral phase of CS mergers are a more promising avenue for identifying twins.

IV. CONCLUSIONS

To summarize, we investigated the impact of two recent observational/experimental results: the inference of the radius of PSR J0740 + 6620 [2,3] from the x-ray data provided by the NICER experiment and that of the neutron skin thickness by the PREX-II experiment in conjunction with the DF analysis of Refs. [13,14], on the static properties of relativistic hybrid stars. The analysis of Ref. [13] gives a value of L_{sym} , which is in potential tension with the TD and radius limits inferred from the GW170817 analysis. The L_{sym} value extracted in the analysis of Ref. [14] is within the accepted range and does not pose any tension with multimessenger astrophysics. The above mentioned new results were confronted here with the conjecture of strong first-order phase transition and the formation of hybrid stars. In doing so, we adopted a density-functional model of nucleonic matter which allows for the accurate description of low-density nuclear phenomenology, along with a flexible parametrization of high-density quark matter. Our main finding is that it is possible

to account for current astrophysical and nuclear experimental constraints within the scenario of hybrid stars, which can appear as twin configurations, with a low value of phase transition density from nucleonic to quark matter. Specifically, in this scenario, the first-order phase transition naturally softens the EOS at intermediate densities (which is required to avoid the potential tension between the GW170817 event and the PREX-II measurement’s interpretation of Ref. [13]), and the assumption of a high sound speed in quark matter stiffens the EOS at high densities, which is required to account for $M \gtrsim 2.0 M_{\odot}$ massive CS and the large radius of PSR J0740 + 6620 (as measured by the NICER analysis teams). We have quantified under which conditions such models may have twin solutions. In particular, for the squared sound speed in quark matter $s = 0.6$ and $s = 1/3$, we find twin stars *and* a large enough maximum mass to allow for a CS in the GW190814 merger event. For low values of s , the range of the difference in the radii for twins expands; for example, $\Delta R_{\text{twin}} \sim 1.0$ km found for $s = 1$ becomes 3 km for $s = 0.6$. In the EOS models where Δ resonances appear (see Refs. [30,59] and references therein), the EOS softens at intermediate densities, and the radius of the star is reduced, with consequences for the M - R relation similar to those found here.

ACKNOWLEDGMENTS

M. A. is supported by the U.S. Department of Energy, Office of Science, Office of Nuclear Physics under Award No. DE-FG02-05ER41375. J.L. is supported by the “Fundamental Research Funds for the Central Universities” under Grant No. SWU-020021. A.S. is supported by the Deutsche Forschungsgemeinschaft (Grant No. SE 1836/5-1) and European COST Action “PHAROS” (CA16214).

-
- [1] H. T. Cromartie, E. Fonseca, S. M. Ransom *et al.* (NANOGrav Collaboration), Relativistic Shapiro delay measurements of an extremely massive millisecond pulsar, *Nat. Astron.* **4**, 72 (2020).
 - [2] T. E. Riley, A. L. Watts, P. S. Ray *et al.*, A NICER view of the massive pulsar PSR J0740 + 6620 informed by radio timing and XMM-newton spectroscopy, *Astrophys. J. Lett.* **918**, L27 (2021).
 - [3] M. C. Miller, F. K. Lamb, A. J. Dittmann *et al.*, The radius of PSR J0740 + 6620 from NICER and XMM-newton data, *Astrophys. J. Lett.* **918**, L28 (2021).
 - [4] B. P. Abbott, R. Abbott, T. D. Abbot *et al.* (LIGO Scientific, Virgo Collaborations), Properties of the Binary Neutron Star Merger GW170817, *Phys. Rev. X* **9**, 011001 (2019).
 - [5] H. Tan, T. Dore, V. Dexheimer, J. Noronha-Hostler, and N. Yunes, Extreme matter meets extreme gravity: Ultra-heavy neutron stars with crossovers and first-order phase transitions, [arXiv:2106.03890](https://arxiv.org/abs/2106.03890).
 - [6] B. Biswas, Bayesian model-selection of neutron star equation of state using multi-messenger observations, [arXiv:2106.02644](https://arxiv.org/abs/2106.02644).
 - [7] I. Legred, K. Chatziioannou, R. Essick, S. Han, and P. Landry, Impact of the PSR J0740 + 6620 radius constraint on the properties of high-density matter, *Phys. Rev. D* **104**, 063003 (2021).
 - [8] G. Raaijmakers, S. K. Greif, K. Hebeler, T. Hinderer, S. Nisanke, A. Schwenk, T. E. Riley, A. L. Watts, J. M. Lattimer, and W. C. G. Ho, Constraints on the dense matter equation of state and neutron star properties from NICER’s

- mass-radius estimate of PSR J0740 + 6620 and multimessenger observations, *Astrophys. J. Lett.* **918**, L29 (2021).
- [9] S. Huth, P. T. H. Pang, I. Tews, T. Dietrich, A. Le Fèvre, W. Trautmann, K. Agarwal, M. Bulla, M. W. Coughlin, and C. Van Den Broeck, Constraining neutron-star matter with microscopic and macroscopic collisions, [arXiv:2107.06229](https://arxiv.org/abs/2107.06229).
- [10] N.-B. Zhang and B.-A. Li, Impacts of NICER's radius measurement of PSR J0740 + 6620 on nuclear symmetry energy at suprasaturation densities, *Astrophys. J.* **921**, 111 (2021).
- [11] S.-P. Tang, J.-L. Jiang, M.-Z. Han, Y.-Z. Fan, and D.-M. Wei, Constraints on the phase transition and nuclear symmetry parameters from PSR J0740 + 6620 and multimessenger data of other neutron stars, *Phys. Rev. D* **104**, 063032 (2021).
- [12] D. Adhikari, H. Albataineh, D. Androic, K. Aniol, D. S. Armstrong *et al.* (PREX Collaboration), Accurate Determination of the Neutron Skin Thickness of ^{208}Pb Through Parity-Violation in Electron Scattering, *Phys. Rev. Lett.* **126**, 172502 (2021).
- [13] B. T. Reed, F. J. Fattoyev, C. J. Horowitz, and J. Piekarewicz, Implications of PREX-2 on the Equation of State of Neutron-Rich Matter, *Phys. Rev. Lett.* **126**, 172503 (2021).
- [14] P.-G. Reinhard, X. Roca-Maza, and W. Nazarewicz, Information Content of the Parity-Violating Asymmetry in ^{208}Pb , *Phys. Rev. Lett.* **127**, 232501 (2021).
- [15] J. M. Lattimer and Y. Lim, Constraining the symmetry parameters of the nuclear interaction, *Astrophys. J.* **771**, 51 (2013).
- [16] P. Danielewicz and J. Lee, Symmetry energy II: Isobaric analog states, *Nucl. Phys.* **A922**, 1 (2014).
- [17] M. Oertel, M. Hempel, T. Klähn, and S. Typel, Equations of state for supernovae and compact stars, *Rev. Mod. Phys.* **89**, 015007 (2017).
- [18] M. Baldo and G. F. Burgio, The nuclear symmetry energy, *Prog. Part. Nucl. Phys.* **91**, 203 (2016).
- [19] M. G. Alford, A. Schmitt, K. Rajagopal, and T. Schäfer, Color superconductivity in dense quark matter, *Rev. Mod. Phys.* **80**, 1455 (2008).
- [20] E. Annala, T. Gorda, A. Kurkela, and A. Vuorinen, Gravitational-Wave Constraints on the Neutron-Star-Matter Equation Of State, *Phys. Rev. Lett.* **120**, 172703 (2018).
- [21] V. Paschalidis, K. Yagi, D. Alvarez-Castillo, D. B. Blaschke, and A. Sedrakian, Implications from GW170817 and I-Love-Q relations for relativistic hybrid stars, *Phys. Rev. D* **97**, 084038 (2018).
- [22] E. R. Most, L. R. Weih, L. Rezzolla, and J. Schaffner-Bielich, New Constraints on Radii and Tidal Deformabilities of Neutron Stars from GW170817, *Phys. Rev. Lett.* **120**, 261103 (2018).
- [23] I. Tews, J. Margueron, and S. Reddy, Critical examination of constraints on the equation of state of dense matter obtained from GW170817, *Phys. Rev. C* **98**, 045804 (2018).
- [24] G. F. Burgio, A. Drago, G. Pagliara, H. J. Schulze, and J. B. Wei, Are small radii of compact stars ruled out by GW170817/AT2017gfo? *Astrophys. J.* **860**, 139 (2018).
- [25] D. E. Alvarez-Castillo, D. B. Blaschke, A. G. Grunfeld, and V. P. Pagura, Third family of compact stars within a nonlocal chiral quark model equation of state, *Phys. Rev. D* **99**, 063010 (2019).
- [26] J.-E. Christian, A. Zacchi, and J. Schaffner-Bielich, Signals in the tidal deformability for phase transitions in compact stars with constraints from GW170817, *Phys. Rev. D* **99**, 023009 (2019).
- [27] G. Montana, L. Tolos, M. Hanauske, and L. Rezzolla, Constraining twin stars with GW170817, *Phys. Rev. D* **99**, 103009 (2019).
- [28] M. Sieniawska, W. Turczanski, M. Bejger, and J. L. Zdunik, Tidal deformability and other global parameters of compact stars with strong phase transitions, *Astron. Astrophys.* **622**, A174 (2019).
- [29] R. Essick, P. Landry, and D. E. Holz, Nonparametric inference of neutron star composition, equation of state, and maximum mass with GW170817, *Phys. Rev. D* **101**, 063007 (2020).
- [30] J. J. Li, A. Sedrakian, and M. Alford, Relativistic hybrid stars with sequential first-order phase transitions and heavy-baryon envelopes, *Phys. Rev. D* **101**, 063022 (2020).
- [31] Z. Miao, A. Li, Z. Zhu, and S. Han, Constraining hadron-quark phase transition parameters within the quark-mean-field model using multimessenger observations of neutron stars, *Astrophys. J.* **904**, 103 (2020).
- [32] A. Li, Z. Miao, S. Han, and B. Zhang, Constraints on the maximum mass of neutron stars with a quark core from GW170817 and NICER PSR J0030 + 0451 data, *Astrophys. J.* **913**, 27 (2021).
- [33] G. Malfatti, M. G. Orsaria, I. F. Ranea-Sandoval, G. A. Contrera, and F. Weber, Delta baryons and diquark formation in the cores of neutron stars, *Phys. Rev. D* **102**, 063008 (2020).
- [34] M. C. Rodriguez, I. F. Ranea-Sandoval, M. Mariani, M. G. Orsaria, G. Malfatti, and O. M. Guilera, Hybrid stars with sequential phase transitions: The emergence of the g_2 mode, *J. Cosmol. Astropart. Phys.* **02** (2021) 009.
- [35] M. G. Alford, S. Han, and M. Prakash, Generic conditions for stable hybrid stars, *Phys. Rev. D* **88**, 083013 (2013).
- [36] M. G. Alford and A. Sedrakian, Compact Stars with Sequential QCD Phase Transitions, *Phys. Rev. Lett.* **119**, 161104 (2017).
- [37] T. E. Riley, A. L. Watts, S. Bogdanov *et al.*, A NICER view of PSR J0030 + 0451: Millisecond pulsar parameter estimation, *Astrophys. J. Lett.* **887**, L21 (2019).
- [38] M. C. Miller, F. K. Lamb, and A. J. Dittmann, PSR J0030 + 0451 mass and radius from NICER data and implications for the properties of neutron star matter, *Astrophys. J. Lett.* **887**, L24 (2019).
- [39] G. A. Lalazisis, T. Niksic, D. Vretenar, and P. Ring, New relativistic mean-field interaction with density-dependent meson-nucleon couplings, *Phys. Rev. C* **71**, 024312 (2005).
- [40] J. J. Li and A. Sedrakian, Constraining compact star properties with nuclear saturation parameters, *Phys. Rev. C* **100**, 015809 (2019).
- [41] J. Margueron, R. H. Casali, and F. Gulminelli, Equation of state for dense nucleonic matter from metamodelling: II. Predictions for neutron star properties, *Phys. Rev. C* **97**, 025806 (2018).
- [42] E. Fonseca, H. T. Cromartie, T. T. Pennucci *et al.*, Refined mass and geometric measurements of the high-mass PSR J0740 + 6620, *Astrophys. J. Lett.* **915**, L12 (2021).

- [43] L. Rezzolla, E. R. Most, and L. R. Weih, Using gravitational-wave observations and quasi-universal relations to constrain the maximum mass of neutron stars, *Astrophys. J. Lett.* **852**, L25 (2018).
- [44] S. Khadkikar, A. R. Raduta, M. Oertel, and A. Sedrakian, Maximum mass of compact stars from gravitational wave events with finite-temperature equations of state, *Phys. Rev. C* **103**, 055811 (2021).
- [45] R. Abbott, T. D. Abbott, S. Abraham *et al.* (LIGO Scientific, Virgo Collaborations), GW190814: Gravitational waves from the coalescence of a 23 solar mass black hole with a 2.6 solar mass compact object, *Astrophys. J. Lett.* **896**, L44 (2020).
- [46] F. J. Fattoyev, C. J. Horowitz, J. Piekarewicz, and B. Reed, GW190814: Impact of a 2.6 solar mass neutron star on the nucleonic equations of state, *Phys. Rev. C* **102**, 065805 (2020).
- [47] J. J. Li, A. Sedrakian, and F. Weber, Rapidly rotating Δ -resonance-admixed hypernuclear compact stars, *Phys. Lett. B* **810**, 135812 (2020).
- [48] J. Estee, W. G. Lynch, C. Y. Tsang *et al.* (S π RIT Collaboration), Probing the Symmetry Energy with the Spectral Pion Ratio, *Phys. Rev. Lett.* **126**, 162701 (2021).
- [49] R. Essick, P. Landry, A. Schwenk, and I. Tews, Astrophysical Constraints on the Symmetry Energy and the Neutron Skin of ^{208}Pb with Minimal Modeling Assumptions, *Phys. Rev. Lett.* **127**, 192701 (2021).
- [50] D. Radice, A. Perego, F. Zappa, and S. Bernuzzi, GW170817: Joint constraint on the neutron star equation of state from multimessenger observations, *Astrophys. J. Lett.* **852**, L29 (2018).
- [51] K. Kiuchi, K. Kyutoku, M. Shibata, and K. Taniguchi, Revisiting the lower bound on tidal deformability derived by AT2017gfo, *Astrophys. J. Lett.* **876**, L31 (2019).
- [52] J. L. Zdunik and P. Haensel, Maximum mass of neutron stars and strange neutron-star cores, *Astron. Astrophys.* **551**, A61 (2013).
- [53] L. Bonanno and A. Sedrakian, Composition and stability of hybrid stars with hyperons and quark color-superconductivity, *Astron. Astrophys.* **539**, A16 (2012).
- [54] D. Blaschke, T. Klahn, R. Lastowiecki, and F. Sandin, How strange are compact star interiors? *J. Phys. G* **37**, 094063 (2010).
- [55] M. G. Alford, K. Rajagopal, S. Reddy, and F. Wilczek, Minimal color-flavor-locked-nuclear interface, *Phys. Rev. D* **64**, 074017 (2001).
- [56] J.-E. Christian and J. Schaffner-Bielich, Supermassive neutron stars rule out twin stars, *Phys. Rev. D* **103**, 063042 (2021).
- [57] D. Gondek, P. Haensel, and J. L. Zdunik, Radial pulsations and stability of protoneutron stars, *Astron. Astrophys.* **325**, 217 (1997), <http://aa.springer.de/papers/7325001/2300217/small.htm>.
- [58] K. Strobel and M. K. Weigel, On the minimum and maximum mass of neutron stars and the delayed collapse, *Astron. Astrophys.* **367**, 582 (2001).
- [59] A. Sedrakian, J.-J. Li, and F. Weber, Hyperonization in compact stars, [arXiv:2105.14050](https://arxiv.org/abs/2105.14050).